Cell, Volume *139*

Supplemental Data

Resource

A Genome-wide RNAi Screen for Modifiers of the Circadian Clock in Human Cells

Eric E. Zhang, Andrew C. Liu, Tsuyoshi Hirota, Loren J. Miraglia, Genevieve Welch, Pagkapol Y. Pongsawakul, Xianzhong Liu, Ann Atwood, Jon W. Huss III, Jeff Janes, Andrew I. Su, John B. Hogenesch, and Steve A. Kay

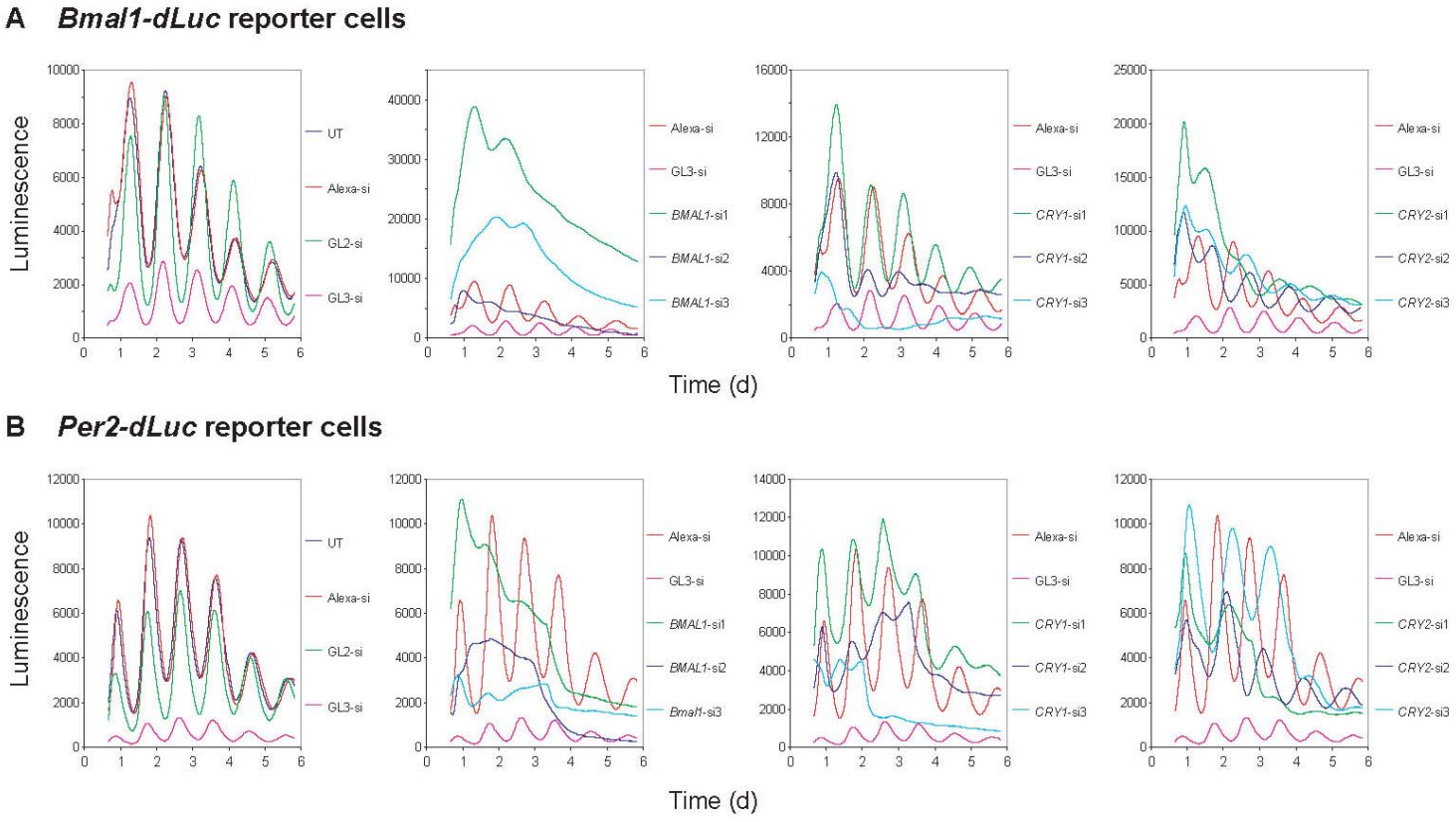

Figure S1. Circadian Reporter Cell Lines.
Two clonal circadian reporter cell lines, *Bmal1-dLuc* (A) and *Per2-dLuc* (B), were established and used in this study. These two cell lines display robust cellular rhythmicity with near anti-phasic oscillation of bioluminescence expression. Upon transfection-mediated siRNA delivery and knockdown of *BMAL1*, *CRY1* or *CRY2*, both

cells displayed similar circadian phenotypes. We chose *BMAL1*-si2, *CRY1*-si2, and *CRY2*-si2 siRNA constructs in this study because they gave rise to cellular clock phenotypes that are consistent with previous results: knockdown of *BMAL1* results in low-amplitude oscillations and loss of rhythmicity, knockdown of *CRY1* leads to shorter period length and rapid damping, and knockdown of *CRY2* results in long period length. The data presented here were from LumiCycle cellular assays in 35-mm dishes. The assay was then adapted to 96-well and 384-well formats for high-throughput screening. UT, untreated with siRNA. Alexa fluo labeled siRNA allows for visualization of transfection efficiency and was used as a control. GL2 and GL3 siRNAs are negative and positive controls for specific targeting of the firefly luciferase in the pGL3 vector series.

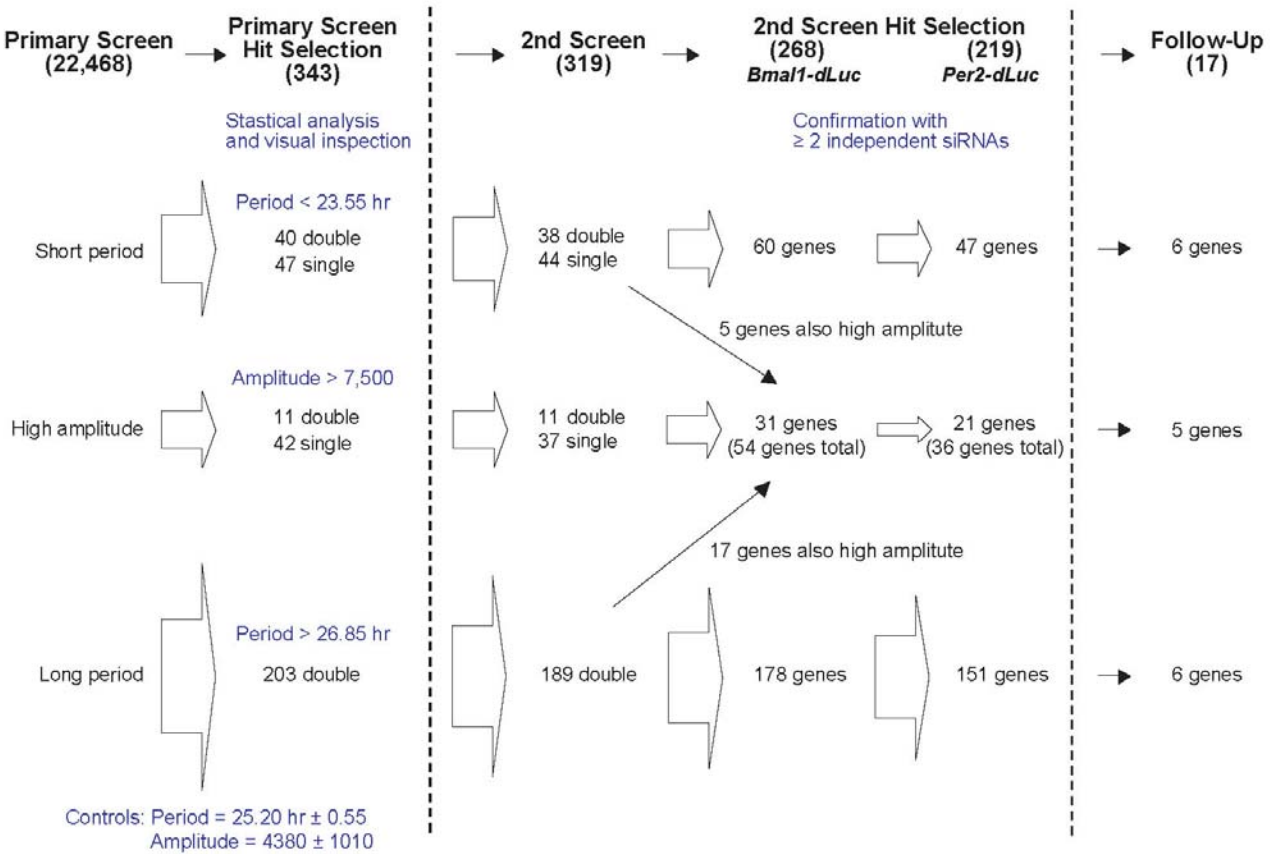

Figure S2. Screen Logic.
Outline of the screen logic of the primary and secondary screens, highlighting criteria for hit selection. A total of 343 hits were selected from the primary screen, among which 319 genes were conducted for the secondary screen, while the rest 24 hits were not tested for technical issues. From the secondary screen, 222 out of 238 double-hitter and 47 out of 83 single-hitter genes were reconfirmed in *Bmal1-dLuc* reporter cells. 17 genes representing the three major cellular clock phenotypes were chosen in the follow-up studies. Note: some of the single hits in primary screen (2 siRNAs/well, 4 siRNAs/gene) were in fact double hits in the secondary screen (1 siRNA/well, ≥4 siRNAs/gene).

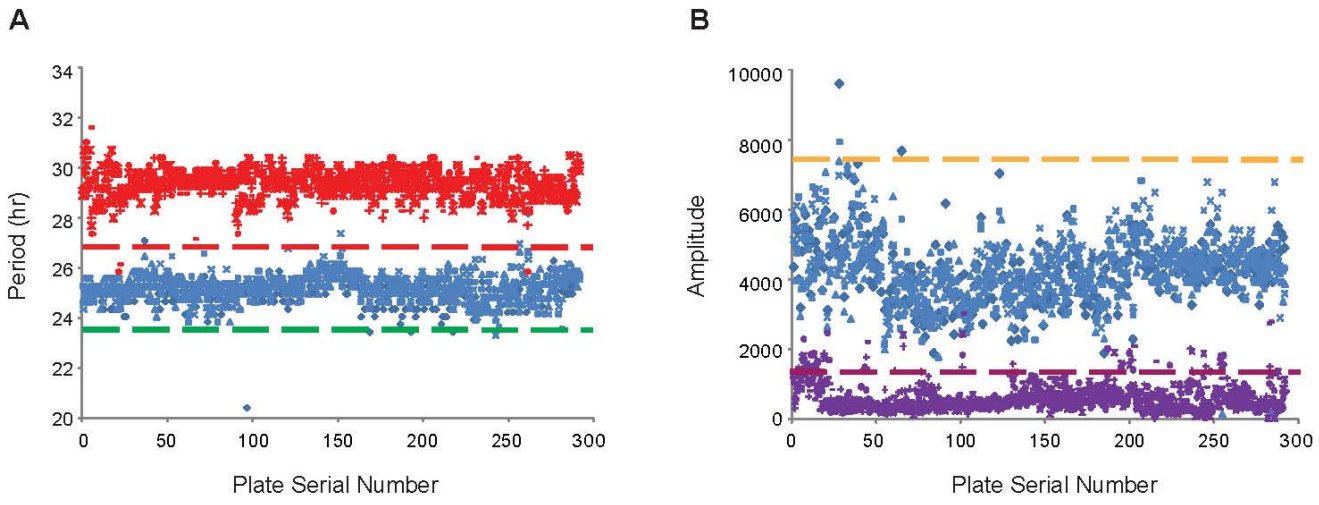

Figure S3. Plate-to-Plate Distribution of Circadian Parameters in Primary Screen.
Data for all control siRNAs from the entire primary screen (4 wells/each control/384-well plate, 292 plates in total) were plotted for period (A) and amplitude (B).
(A) Period distribution. The period distribution for negative control wells (GL2, blue) is 25.20 hr ± 0.55 (n = 1176). *CRY2* siRNA (red) served as a positive control for period alteration (29.43 hr ± 0.65, n = 1176). Red and green dashed lines indicate upper limit and lower limit, respectively, with each representing three standard deviations from the control population and serving as the cut-off for long and short periods.
(B) Amplitude distribution. The distribution of negative control wells (blue) is 4380 ± 1010, and that of *BMAL1* siRNA (purple) is 692 ± 626 (n = 1176). Yellow dashed line indicates upper limit of three standard deviations from the control population and serves as the cut-off for high-amplitude hits. Purple line indicates upper limit of one standard deviation from the *BMAL1* siRNA population and serves as the cut-off for arrhythmic wells.

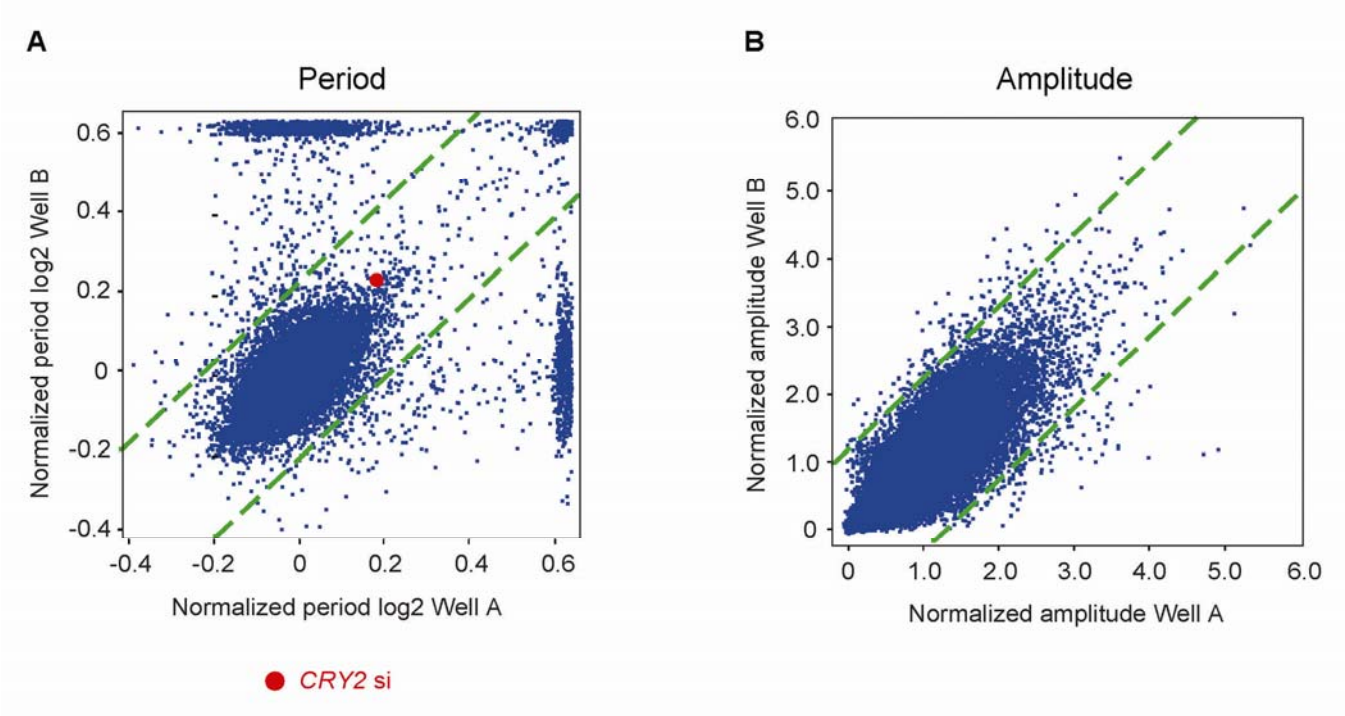

Figure S4. Screen Noise Distribution of Circadian Parameters in Primary Screen. Overview of data distribution in period length (A) and rhythm amplitude (B) between replicates in the primary screen. Raw data were first divided by the mean of the entire screen. The normalized period length or amplitude from one experiment was plotted against the corresponding replicate experiment. Screen noise was defined as one standard deviation from the mean (green dash-lines), and dots located beyond screen noise were filtered out from further analysis. For both period length and amplitude, the majority of hits (>95.6% and >99.2%, respectively) showed consistent data among replicates. The inconsistency for period length resulted mainly from poor curve fitting of data due to for example low-amplitude oscillations.

A

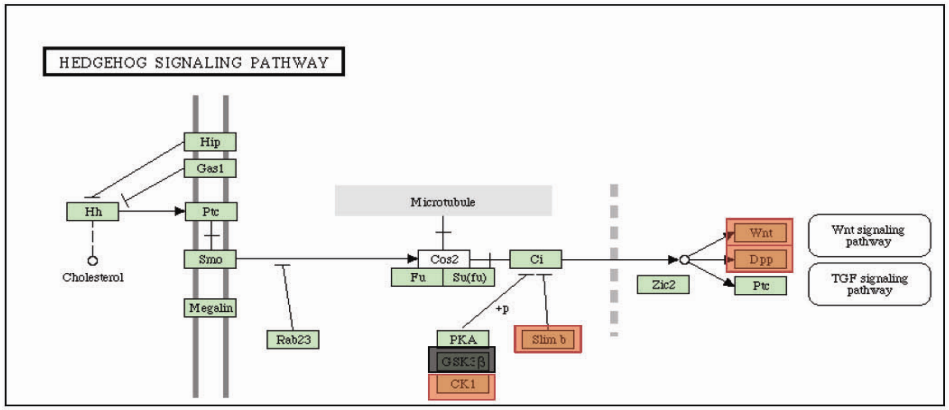

B

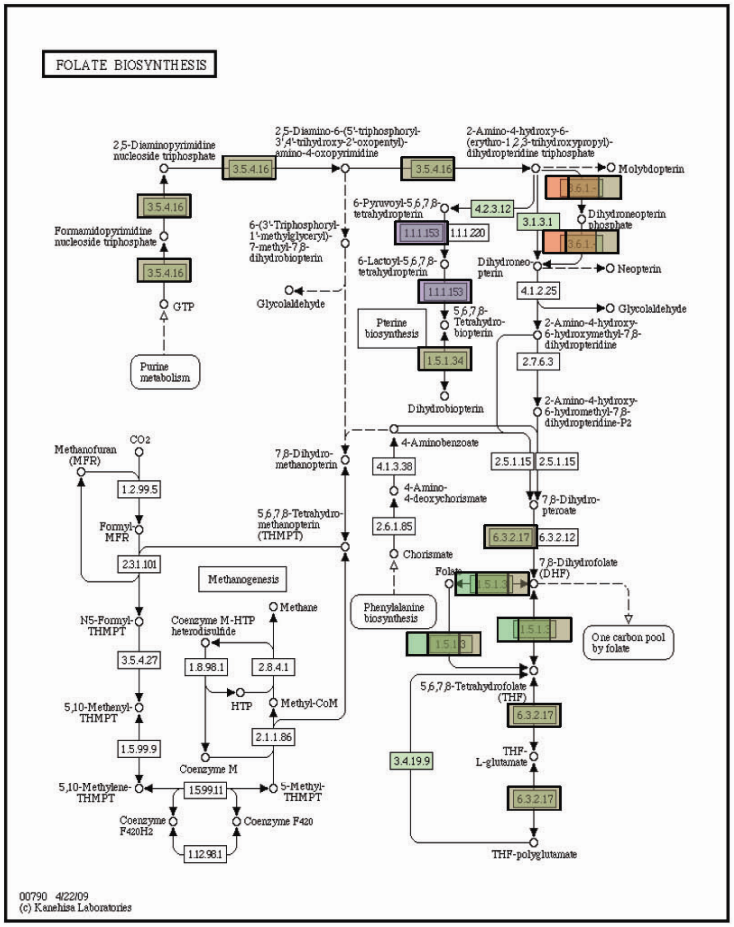

C

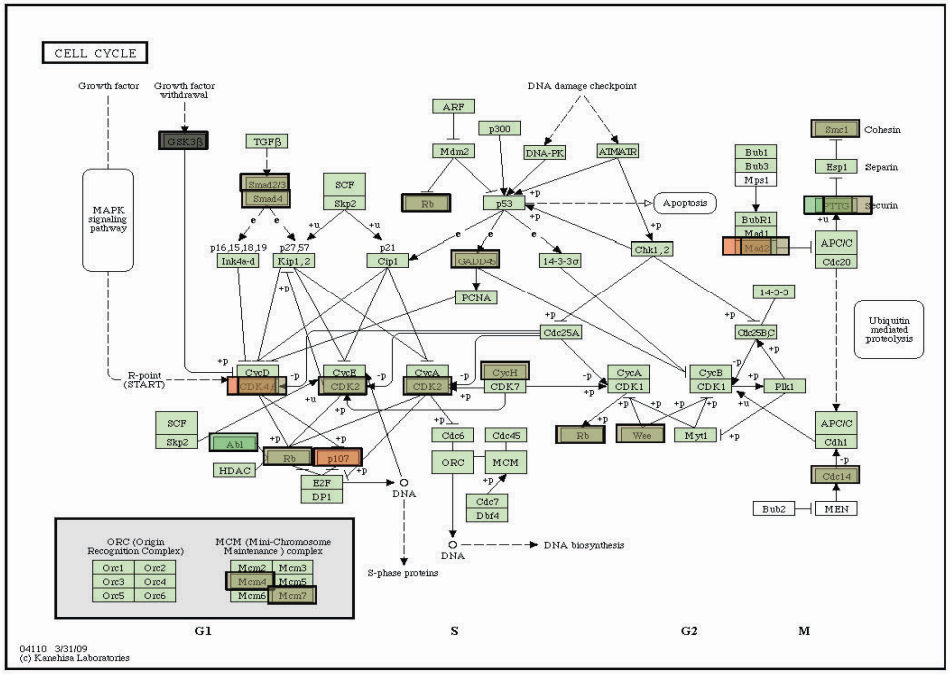

Short Period

Long period

High amplitude

Cycles in Liver

Implicated in Clock

Figure S5. Pathway Analysis with Primary Screen Hits.
Pathway analysis was performed using NIH David Pathway Analysis tool. The 343 gene hits uncovered in the primary screen were used for this analysis. Pathway analysis revealed an overrepresentation of several pathways including insulin signaling (Figure 6A), the hedgehog pathway (A), the cell cycle (B), and folate metabolism (C). The components in the canonical pathways are framed and/or shaded. The highlighted genes were either known to be implicated in clock function or found as cellular clock regulators in our screen.

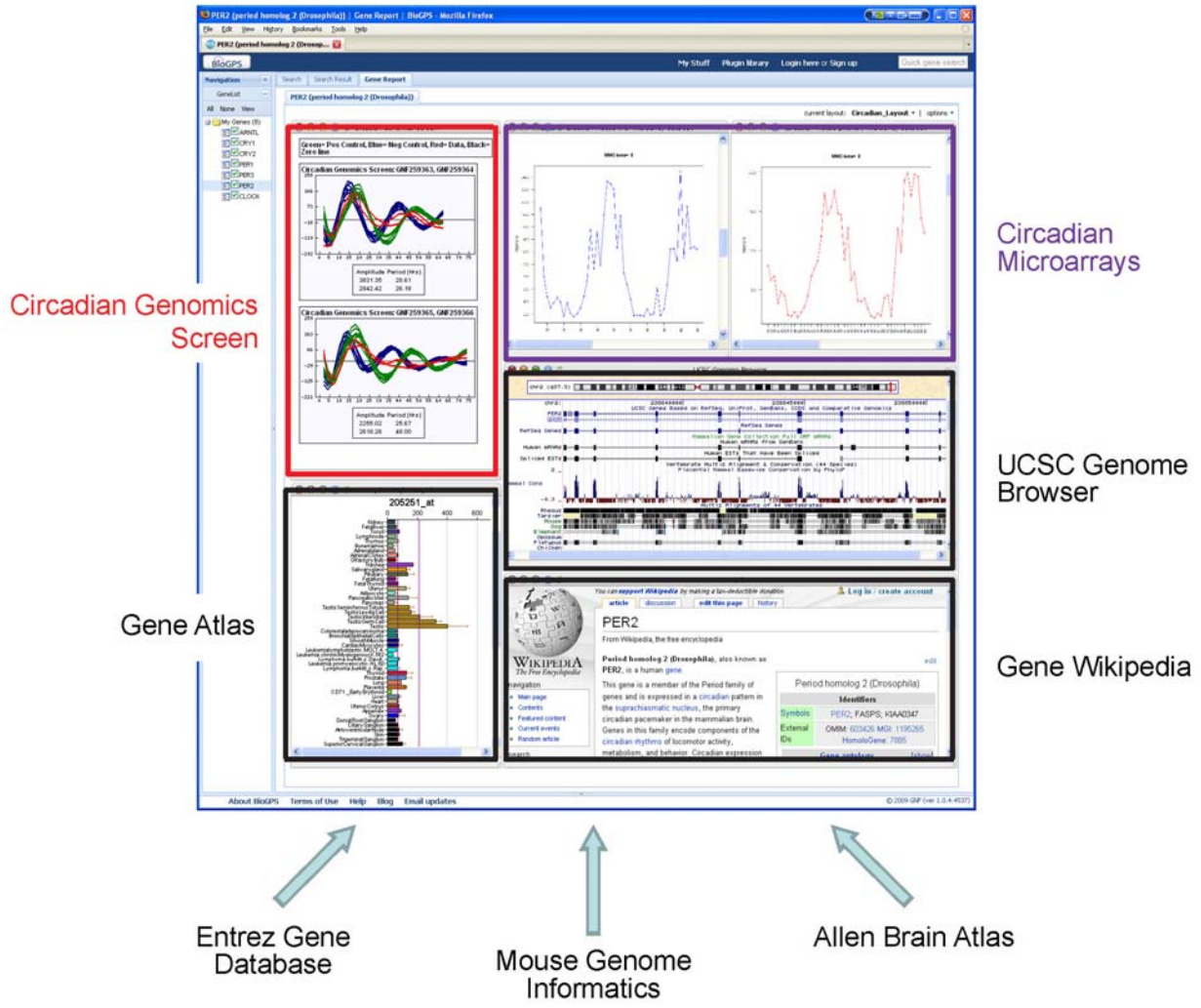

Figure S6. Overview of Web-Based Data Resource in Circadian BioGPS.
We built a database (http://biogps.gnf.org/circadian/) to visualize and explore the primary screening data. The respective circadian parameters are displayed (highlighted in the red box). In addition, circadian microarray data from mouse liver and pituitary are displayed in separated windows (purple box). These databases are linked to multiple online resources including the UCSC Genome Browser, Tissue Atlas Gene Expression database, and Gene Wikipedia, which describes the expanded annotation for searched genes (e.g., *PER2* is shown). Furthermore, BioGPS provides a platform for building customized layouts that integrate other web-based resources such as Entrez Gene, Mouse Genome Informatics, and the Allen Brain Atlas.

Table S2. List of clock protein interactions with primary hits

Color coding	clock genes
	high amplitude
	short period
	long period

A. Direct Interaction

Clock Ref	Clock Symbol	Hit Ref	Hit Symbol
NM_001178	ARNTL	NM_022470	ZMAT3
NM_002616	PER1	NM_013314	BLNK
NM_002616	PER1	NM_015179	RRP12

B. "One-Molecule-Intermediated" Interaction

Clock Ref	Clock Symbol	Interactant Ref	Interactant Symbol	Hit Ref	Hit Symbol
NM_001178	ARNTL	XM_374491	PPP1R9A	NM_018067	MAP7D1
NM_001178	ARNTL	NM_021009	UBC	NM_006142	SFN
NM_001178	ARNTL	NM_003884	PCAF	NM_000059	BRCA2
NM_001178	ARNTL	NM_003884	PCAF	NM_003496	TRRAP
NM_001178	ARNTL	NM_002957	RXRA	NM_002434	MPG
NM_001178	ARNTL	NM_001530	HIF1A	NM_003968	UBE1C
NM_001178	ARNTL	NM_001530	HIF1A	NM_017902	HIF1AN
NM_001178	ARNTL	NM_001530	HIF1A	NM_015179	RRP12
NM_001178	ARNTL	NM_005348	HSP90AA1	NM_177559	CSNK2A1
NM_001178	ARNTL	NM_005348	HSP90AA1	NM_005334	HCFC1
NM_004898	CLOCK	NM_015641	TES	NM_005697	SCAMP2
NM_004898	CLOCK	NM_153260	FLJ36812	NM_020772	NUFIP2
NM_004898	CLOCK	XM_377778	LOC402110	NM_005334	HCFC1
NM_004898	CLOCK	NM_002835	PTPN12	NM_001424	EMP2
NM_004898	CLOCK	NM_020183	ARNTL2	NM_001430	EPAS1
NM_002518	NPAS2	NM_003884	PCAF	NM_000059	BRCA2
NM_002518	NPAS2	NM_003884	PCAF	NM_003496	TRRAP
NM_002518	NPAS2	NM_002957	RXRA	NM_002434	MPG
NM_002518	NPAS2	NM_181659	NCOA3	NM_001556	IKBKB
NM_002616	PER1	XM_290629	C14ORF78	NM_014258	SYCP2
NM_002616	PER1	NM_002468	MYD88	NM_016166	PIAS1
NM_002616	PER1	NM_014676	PUM1	NM_018067	MAP7D1
NM_002616	PER1	NM_013333	EPN1	NM_005826	HNRPR
NM_002616	PER1	XM_290629	C14ORF78	NM_001281	TBCB
NM_002616	PER1	NM_021906	USP9X	NM_004697	PRPF4
NM_002616	PER1	NM_006346	C13ORF24	NM_006609	MAP3K2
NM_002616	PER1	NM_015638	TRPC4AP	NM_005781	TNK2
NM_002616	PER1	NM_000249	MLH1	NM_001430	EPAS1
NM_002616	PER1	NM_021906	USP9X	NM_002866	RAB3A
NM_002616	PER1	XM_290629	C14ORF78	NM_017838	NOLA2
NM_002616	PER1	NM_014676	PUM1	NM_002866	RAB3A
NM_002616	PER1	NM_006346	C13ORF24	NM_006210	PEG3
NM_002616	PER1	NM_015927	TGFB1I1	NM_013390	TMEM2
NM_002616	PER1	NM_021906	USP9X	NM_133370	YT521
NM_022817	PER2	NM_001895	CSNK2A1	NM_005953	MT2A
NM_022817	PER2	NM_001895	CSNK2A1	NM_004327	BCR
NM_022817	PER2	NM_178552	MGC35206	NM_018449	UBAP2
NM_022817	PER2	NM_004572	PKP2	NM_014515	CNOT2
NM_022817	PER2	NM_003906	MCM3AP	NM_006082	KALPHA1
NM_016831	PER3	NM_002616	PER1	NM_013314	BLNK
NM_016831	PER3	NM_002616	PER1	NM_015179	RRP12
NM_016831	PER3	NM_020765	RBAF600	NM_002532	NUP88
NM_004075	CRY1	NM_021138	TRAF2	NM_002460	IRF4
NM_004075	CRY1	NM_021105	PLSCR1	NM_005157	ABL1
NM_004075	CRY1	NM_021138	TRAF2	NM_001556	IKBKB
NM_021117	CRY2	NM_006247	PPP5C	NM_001316	CSE1L
NM_005126	NR1D2	NM_177996	EPB41L1	NM_017920	URG4
NM_021724	NR1D1	NM_005087	FXR1	NM_018449	UBAP2
NM_021724	NR1D1	NM_005087	FXR1	NM_017761	PNRC2
NM_005126	NR1D2	NM_001222	CAMK2G	NM_005781	TNK2
NM_005126	NR1D2	NM_005791	MPHOSPH10	NM_018360	CXORF15
NM_006914	RORB	NM_014071	NCOA6	NM_003259	ICAM5
NM_006914	RORB	NM_003388	CYLN2	NM_001894	CSNK1E
NM_001893	CSNK1D	XM_290629	C14ORF78	NM_014258	SYCP2
NM_001893	CSNK1D	XM_290629	C14ORF78	NM_001281	TBCB
NM_001893	CSNK1D	NM_181870	DVL1	NM_001895	CSNK2A1
NM_001893	CSNK1D	NM_004423	DVL3	NM_001895	CSNK2A1
NM_001893	CSNK1D	XM_290629	C14ORF78	NM_017838	NOLA2
NM_001894	CSNK1E	NM_181523	PIK3R1	NM_013314	BLNK
NM_001894	CSNK1E	NM_000546	TP53	NM_000059	BRCA2
NM_001894	CSNK1E	NM_000546	TP53	NM_006142	SFN
NM_001894	CSNK1E	NM_000546	TP53	NM_005157	ABL1
NM_001894	CSNK1E	NM_000546	TP53	NM_004327	BCR
NM_001894	CSNK1E	NM_000546	TP53	NM_000791	DHFR
NM_001894	CSNK1E	NM_000546	TP53	NM_001261	CDK9
NM_001894	CSNK1E	NM_000546	TP53	NM_139046	MAPK8
NM_001894	CSNK1E	NM_000546	TP53	NM_005381	NCL
NM_001894	CSNK1E	NM_003502	AXIN1	NM_001892	CSNK1A1
NM_001894	CSNK1E	NM_032421	CYLN2	NM_014117	PRO0149
NM_001894	CSNK1E	NM_181870	DVL1	NM_001895	CSNK2A1
NM_001894	CSNK1E	NM_004422	DVL2	NM_001895	CSNK2A1

Table S3. siRNAs from Qiagen

	Qiagen catalog number	
HCFC1	Hs_HCFC1_1	Hs_HCFC1_2
POLR3F	Hs_POLR3F_2	Hs_POLR3F_4
PRPF4	Hs_PRPF4_2	Hs_PRPF4_4
SEC13	Hs_SEC13L1_1	Hs_SEC13L1_2
UNC119	Hs_UNC119_1	Hs_UNC119_3
ZMAT3	Hs_WIG1_2	Hs_WIG1_3
ACSF3	Hs_LOC197322_2	Hs_LOC197322_3
B4GALT2	Hs_B4GALT2_2	Hs_B4GALT2_3
CECAM21	Hs_R29124_1_1	Hs_R29124_1_2
TBCB	Hs_CKAP1_2	Hs_CKAP1_3
MPG	Hs_MPG_3	Hs_MPG_2
SELO	Hs_SELO_2	Hs_SELO_3
COX4NB	Hs_NOC4_1	Hs_NOC4_4
FHIT	Hs_FHIT_1	Hs_FHIT_2
HIST1H1B	Hs_HIST1H1B_3	Hs_HIST1H1B_4
NMNAT1	Hs_NMNAT1_3	Hs_NMNAT1_4
PDE1B	Hs_PDE1B_1	Hs_PDE1B_2
	Hs_PDE1B_3	Hs_PDE1B_4
FBXL3	Hs_FBXL3_1	Hs_FBXL3_2
	Hs_FBXL3_4	Hs_FBXL3_5

Table S6. Q-PCR primer sequence

	Fw	Rv
GAPDH	TGCACCACCAACTGCTTAGC	ACAGTCTTCTGGGTGGCAGTG
HCFC1	GGGACATTCCCATCACTTACG	GGTGTCAATATCTAGGGTCCACA
POLR3F	ATCTGCGAATTGGGAATCAG	GATTGGATTGACTGCCCTGT
PRPF4	CTGTCTCCTTGGACCCAAAA	GAACGGTCATAGCAGGTGGT
SEC13	CGTGTGTTCATTTGGACCTG	CCTTCCACAGGGTCACCTTA
UNC119	GATCCGCCACCCGTATGAG	TCTGCTTTATTGTGCATCACCA
ZMAT3	CTGGAGGAGCTATGTAAGCCC	CACATTGCTCATTCTAGCAGGA
ACSF3	CCTGGATGGCTGGTTTAAGA	GCTGACCTTGTAGCCTCCAG
B4GALT2	TCATCTTCAGCGATGTGGAC	GCCTGACACACCTCCAAAGT
CECAM21	CCAACCCAGTCAGCTCCAAC	GCCACCAGAAGACTCCCAAC
TBCB	GTGACCGTTTTCATCAGCAGC	GAACTTGTCGTCAACTCCATACA
MPG	GGGTTGGAGTTCTTCGACCAG	CTCGGAGTTCTGTGCCATTAGG
SELO	GGTCAAGCATCCGGGAGTTTC	AACACAACCGTGCATTGTTCA
COX4NB	GCGCTCATCATGGTAGACAA	GAGATCCTCTGTGCCTCTGG
FHIT	GCCAACATCTCATCAAGCCCT	TGGGTCGTCTGAAACAAATCG
HIST1H1B	CTAAGGAGCGCAATGGCCTTT	CCTTCTTCGGAGTCTTCTTCACT
NMNAT1	TCTCCTTGCTTGTGGTTCATTC	TGACAACTGTGTACCTTCCTGT
PDE1B	AAGCAGTGGTTGGTCCACAG	GTGGAAGTGCGGTCACAGAG
ACTB	CATGTACGTTGCTATCCAGGC	CTCCTTAATGTCACGCACGAT
BMAL1	GCCCATTGAACATCACGAGTAC	CCTGAGCCTGGCCTGATAGTAG
CLOCK	GGCACCACCCATAATAGGGTA	TGTTGCCCCTTAGTCAGGAAC
PER1	TCTGTAAGGATGTGCATCTGGT	CAGGCAGTTGATCTGCTGGT
PER2	AGTTGGCCTGCAAGAACCAG	ACTCGCATTTCCTCTTCAGGG
CRY1	ACAGGTGGCGATTTTTGCTTC	TCCAAAGGGCTCAGAATCATACT
CRY2	CGTGTTCCCAAGGCTGTTCA	CTCCGTCACTACTTCCACACC
NR1D1	TGGACTCCAACAACAACACAG	GTGGGAAGTAGGTGGGACAG
DBP	GTTGATGACCTTTGAACCCGA	CCTCCGGCACCTGGATTTTT
FBXL3	GAGCAGCTGTCCTCATGTCTC	CAATGCAAGTAACAACTCATCACTC